

Supporting Information for

**Sulfate-based Anionic Diblock Copolymer Nanoparticles
for Efficient Occlusion within Zinc Oxide**

Y. Ning, L. A. Fielding, T. S. Andrews, D. J. Gowney, S. P. Armes*

Department of Chemistry, University of Sheffield, Brook Hill, Sheffield, South Yorkshire, S3
7HF, UK.

* Author to whom correspondence should be addressed (S.P.Armes@sheffield.ac.uk).

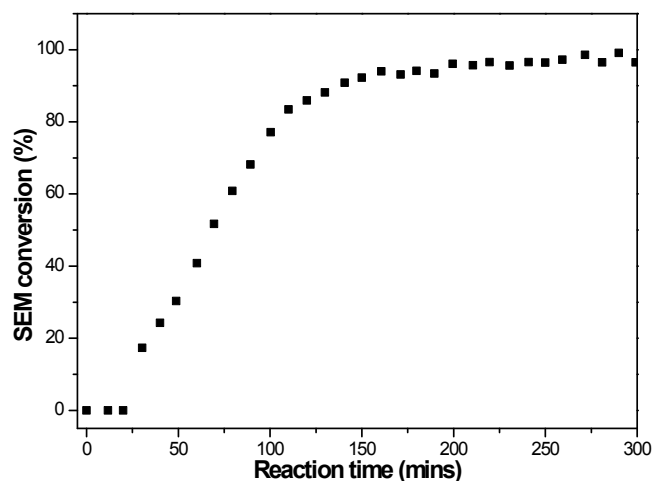


Figure S1. Conversion vs time curve calculated from ^1H NMR spectra (D_2O) for the RAFT synthesis of PSEM macro-CTA in water at 70°C (target DP = 60; CTA/initiator molar ratio = 5.0).

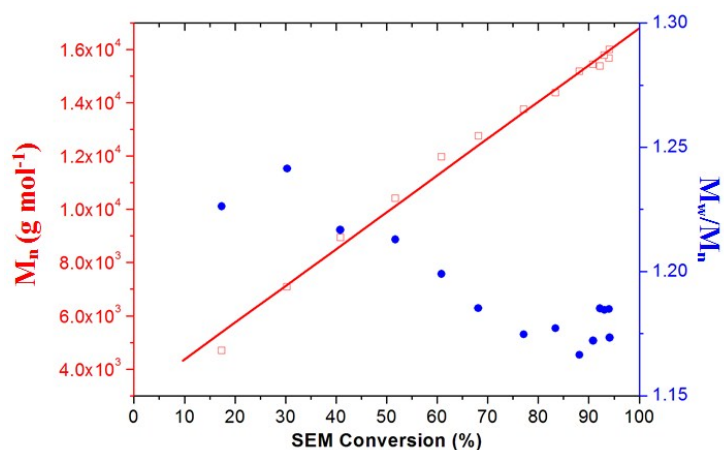


Figure S2. Evolution of the number-average molecular weight M_n (calculated using PEO standards) and polydispersity (M_w/M_n) of PSEM macro-CTA (target DP = 60; CTA/initiator molar ratio = 5.0) with monomer conversion as judged by aqueous GPC.

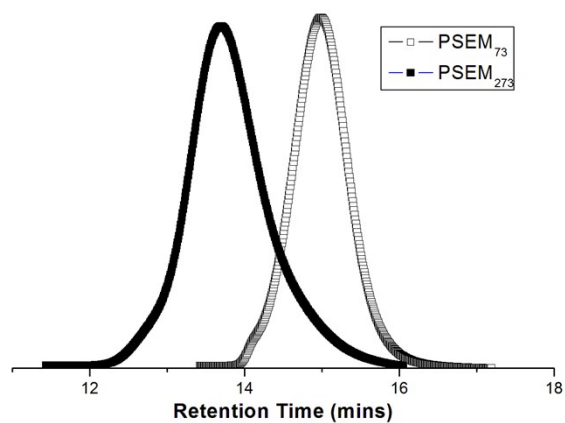


Figure S3. Aqueous GPC curves demonstrating the successful chain extension of PSEM_{73} using SEM monomer. This ‘self-blocking’ experiment was conducted in aqueous solution at 70 °C using ACVA initiator (PSEM_{73} macro-CTA/ACVA molar ratio = 5.0). This demonstrates high blocking efficiency for this PSEM_{73} macro-CTA, which implies high RAFT chain-end fidelity.

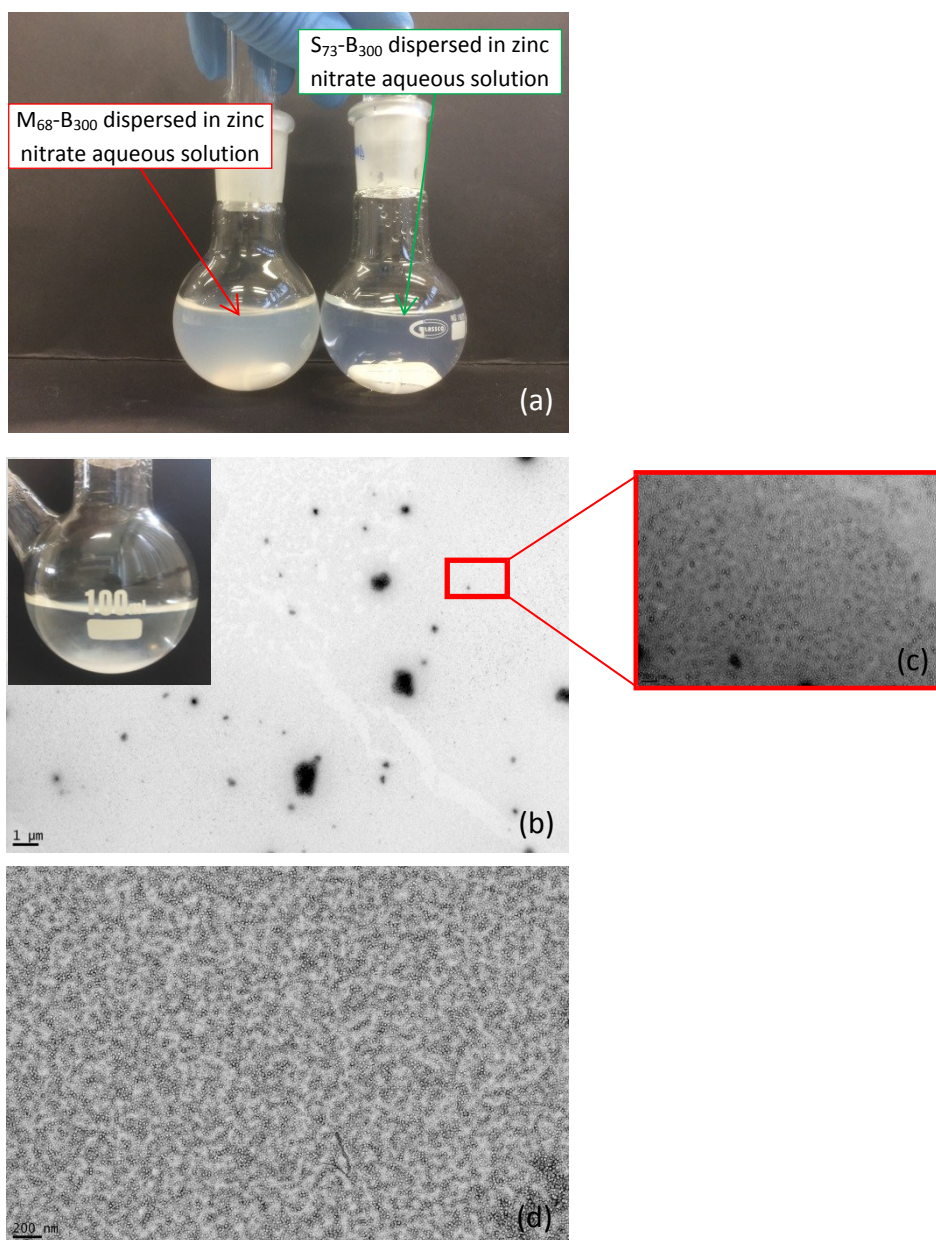


Figure S4. (a) Digital photograph recorded for 0.50 g dm^{-3} M₆₈-B₃₀₀ and 0.50 g dm^{-3} S₇₃-B₃₀₀ dispersed in aqueous zinc nitrate solution; (b) TEM images obtained for 0.50 g dm^{-3} S₃₂-B₃₀₀ nanoparticles dispersed in aqueous zinc nitrate solution (inset shows the corresponding digital photograph); (c) magnified image of the area shown in image (b); (d) TEM images of 0.50 g dm^{-3} S₇₃-B₃₀₀ nanoparticles dispersed in aqueous zinc nitrate solution. A white precipitate was formed immediately on addition of S₃₂-B₃₀₀, but a stable homogeneous aqueous dispersion is maintained for long time periods (months) in the presence of S₇₃-B₃₀₀ nanoparticles.

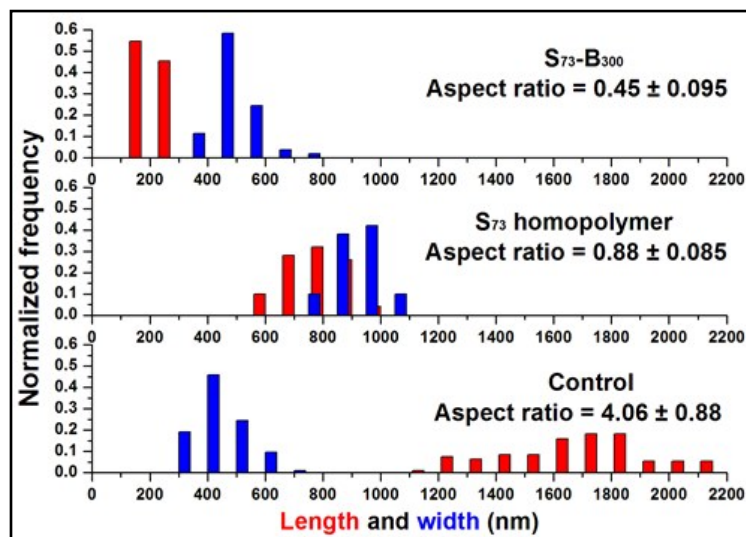


Figure S5. Histograms of the length and width comparison for the samples prepared in the absence of any additive (Control), S_{73} homopolymer, and $S_{73}\text{-B}_{300}$ nanoparticle.

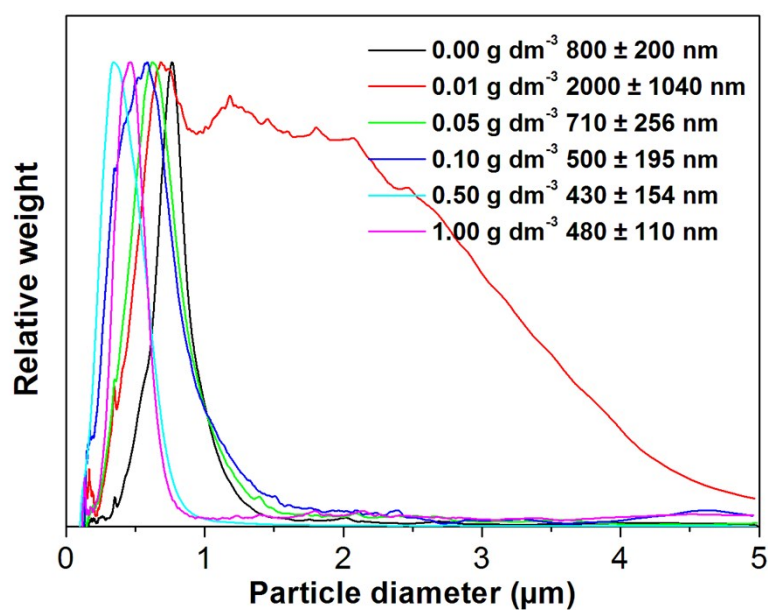


Figure S6. Weight-average particle diameters obtained for ZnO particles prepared in the presence of various concentrations of $S_{73}\text{-B}_{300}$ copolymer nanoparticles, as determined by disk centrifuge photosedimentometry.

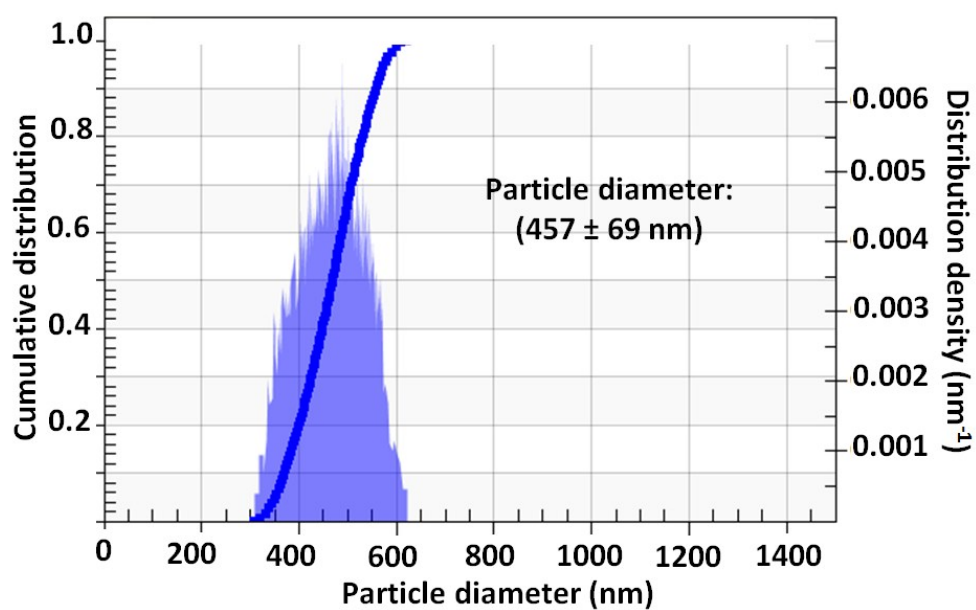


Figure S7. Volume-average particle size distribution determined for the S₇₃-B₃₀₀/ZnO nanocomposite before calcination, as determined by analytical centrifugation (LUMiSizer® instrument).

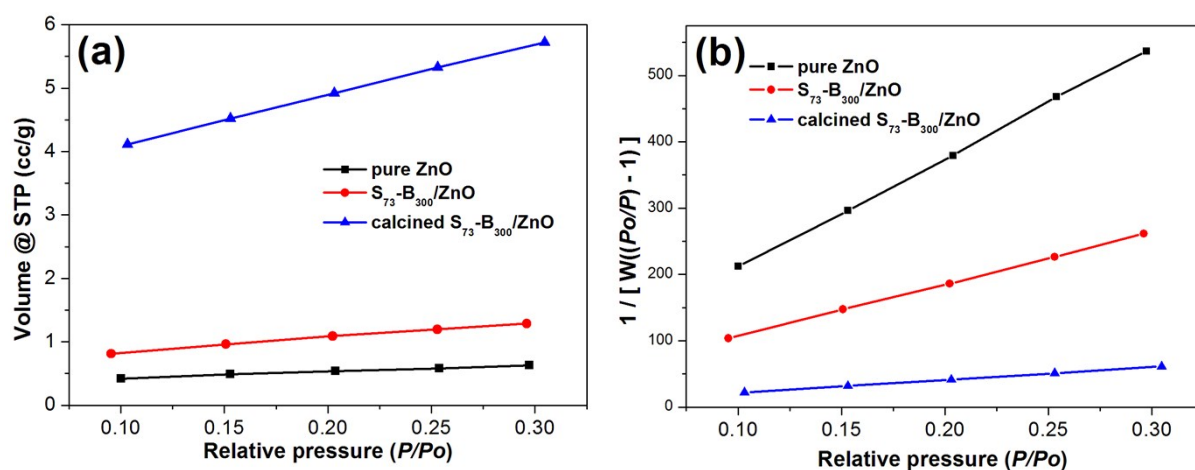


Figure S8. (a) Adsorbed volume of N_2 gas versus relative pressure (P/P_o) ranging from 0.10 to 0.30; (b) Linear BET plots of $1/[W(P_o/P)-1]$ versus P/P_o ranging from 0.10 to 0.30.

The BET surface area of the pure ZnO, $S_{73}\text{-B}_{300}/\text{ZnO}$ and calcined $S_{73}\text{-B}_{300}/\text{ZnO}$ was calculated by N_2 adsorption (Nova 1000e instrument, Quantachrome). All samples were degassed at 40 °C overnight prior to measurements. The specific surface area (in $\text{m}^2 \text{g}^{-1}$) was determined using the five-point BET method over a relative pressure (P/P_o) range of 0.10–0.30.

Table S1. Comparison of copolymer contents determined from TGA and carbon microanalyses.

	wt. %	vol. %
TGA	23	56
Carbon microanalysis	25	58